Indonesian Journal of Biotechnology

VOLUME 28(1), 2023, 37-45 | RESEARCH ARTICLE

Biophysical characterization of folded state type II luciferase-like monooxygenase

Adinda Fitri Salsabila[1], Abidah Tauchid[1], Muhammad Saifur Rohman[1,*], Donny Widianto[1], Sebastian Margino[1]

Department of Agricultural Microbiology, Faculty of Agriculture, Jl. Flora, Kompleks Bulaksumur, Universitas Gadjah Mada, Yogyakarta 55281, Indonesia

*Corresponding author: saifur@ugm.ac.id

SUBMITTED 27 June 2022 **REVISED** 18 September 2022 **ACCEPTED** 9 December 2022

ABSTRACT We noticed that the *Priestia megaterium* genome contains five Luciferase-like monooxygenase (LLM) encoding genes, however, their functions are unknown. The objective of this work was to characterize the biophysical properties of the recombinant LLM2 from *Priestia megaterium* PSA10 through *in vitro* and *in silico* approaches. We successfully cloned into the pET vector system and expressed the recombinant LLM2 in *Escherichia coli* BL21(DE3). The recombinant LLM2 was overproduced and purified in the form of an inclusion body with a molecular weight of ±39.5 kDa when it was analyzed in 15% SDS-PAGE. The inclusion body of recombinant LLM2 was then refolded and characterized for its biophysical properties by measuring the UV spectrum of 200 to 250 nm wavelength and determining the change of enthalpy (ΔH) and entropy (ΔS) at the melting temperature. The refolded recombinant LLM2 exhibited a strong spectrum at 205 nm, while the unfolded recombinant LLM2 did not. The T_m, ΔH_{Tm}, and ΔS_{Tm} values of the refolded recombinant LLM2 were determined to be 318.31±4.4 K, 11.76±1.3 kJ.mol^{-1}, and (3.74±0.48)x10^{-2} kJ.mol^{-1}.K^{-1}, respectively. The predicted 3D structure of LLM2 showed that the protein contains the TIM-barrel, resembling the common global fold of bacterial luciferases. Determination of the cofactor preference suggested that the LLM2 preferred FAD for its cofactor.

KEYWORDS Thermodynamic; TIM-barrel; Flavoenzyme; Flavin Mononucleotide (FMN); Flavin Adenine Dinucleotide (FAD)

1. Introduction

Luciferase-like monooxygenase (LLM) is flavine dependent monooxygenase enzyme (FMO) that belongs to the group of flavine-dependent enzymes (flavoenzymes). Flavoenzyme is an enzyme whose activity requires flavin mononucleotide (FMN) or flavin adenin dinucleotide (FAD) as a cofactor (Romero et al. 2018; Joosten and van Berkel 2007; Hefti et al. 2003). Flavoenzymes composes of diverse enzymes and therefore the enzyme involves in various biological functions such as catabolism, detoxification, and biosynthesis (Hefti et al. 2003; Joosten and van Berkel 2007). One of the most interesting members of flavoenzyme is flavin-dependent monooxygenase (FMO)(Joosten and van Berkel 2007). FMO also has large members of enzymes that catalyze a wide variety of chemo-, regio-, enantioselectivity, hydroxylation, Baeyer-Villiger oxidation, N-hydroxylation, epoxidation, and sulfoxidation reactions (MacHeroux et al. 2011; Huijbers et al. 2017). In addition to oxygen atom incorporation, the enzyme also performs the catalytic reaction; such as halogenation, dehalogenation, denitration, decarboxylation, desulfurization, and light-emitting reactions (Huijbers et al. 2017; van Berkel et al. 2006). Based on their structural features, protein sequence motif, electron donor, and type of oxygenation reaction, FMO is classified into six groups, namely groups A,B, C, D, E, and F (Pimviriyakul and Chaiyen 2020; Huijbers et al. 2017; van Berkel et al. 2006). The member of group A-B has the characteristic of a single component enzyme, meaning that the reduction and oxidation (redox) have been done by the same component of the molecule and rely on the NAD(P)H as an external electron donor. The member of group C-F is distinguished by the requirement of the reductase partner to reduce the flavin cofactor (Huijbers et al. 2017). Among the group, group C has a unique fold of the protein known as the TIM-Barrel fold. One of the important and most studies of group C is bacterial luciferase. Bacterial luciferase is remarkably distinguished by its ability to transform chemical energy into photon visible light (Tinikul et al. 2020).

Luciferase-like monooxygenase (LLM) has a similar fold to common bacterial luciferase and therefore it belongs to group C of FMO. However, no evidence shows that LLM can emit the light during its catalytic activity. It has been reported that LLM performed as various catalytic reactions, such as Baeyer-Villiger oxidation, a reaction that catalyzes the formation of ester from ketone or lactone

from a cyclic ketone (Fürst et al. 2019; Renz and Meunier 1999; Krow 1993). One example of the Baeyer-Villiger oxidation reaction that can be performed by the LLM is MsnO8 from *Streptomyces bottropensis*. The MsnO8 is important for the biosynthesis of mensacarcine, particularly for catalyzing the epoxidation of the mensacarcine to form the epoxide side chain which functions for anticancer activity (Maier et al. 2014).

In addition to the unique conformational fold, most of the member of group C of FMO, use flavin mononucleotide (FMN) as a cofactor to drive the catalysis processes and requires a counterpart protein to reduce the flavin cofactor. The reduced flavin has been converted into an oxidized one through the formation of transiently stable flavin C4a-oxygen adduct (Peroxyflavin or Hydroperoxyflavin). The (hydro)peroxyflavin reacts with electrophilic or nucleophilic substrates to form flavin C4a-hydroxide and followed by releasing water molecules to produce the oxidized flavin (Romero et al. 2018; Chaiyen et al. 2012; Massey 1994; Ghisla and Massey 1989). So far the activation of the flavin molecule only focuses on the C4a atoms of the isoalloxazine ring of flavin. Recently, it has been reported that the N5 atom also functions as an alternative catalytic center (Beaupre and Moran 2020).

Recently, we have noticed that the *Priestia megaterium* DSM319 genome contained five open reading frames of LLM and designated as type I, II, III, IV, and V by *in silico* study (Rohman 2022). However, there is no report regarding the role and function of these LLMs in the cell. In this report, we have cloned, expressed, and characterized the biophysical properties of recombinant type II LLM (LLM2) from *Priestia megaterium* PSA10. Boiphysical properties characterization of refolded recombinant LLM2 could show whether the stable refolded protein could be obtained by *in vitro* refolding.

2. Materials and Methods

2.1. Bacterial cells and genome preparation

For genomic preparation, *Priestia megaterium* PSA10 was cultivated in Luria Bertani medium for 48 hours at room temperature. On the following day, the cell was harvested by centrifugation at 8,000 g for 10 min. The cell pellet was then collected and further subjected for the genomic isolation procedure. Bacterial genomic was prepared by using Wizard Genomic Isolation Kit (Promega). *Escherichia coli* BL21(DE3) (F – *omp*T *hsd*SB (rB- mB-) *gal dcm* (DE3))(Sigma-Aldrich) and pET28a(+) (AddGene) were used as host and vector for recombinant protein expression, respectively. This protocol was similar to the previous study with modification (Pradani et al. 2020).

2.2. Type II luciferase-like monooxygenase (LLM2) open reading frame isolation and cloning

To amplify the LLM2 open reading frame from *P. megaterium* PSA10 genome, the following primer was designed based on the sequence of the LLM2 open reading frame (orf) from *P. megaterium* DSM319 (Acc. No. CP001982). The sequence of the primers was LLM2_F: 5'ATATACCATGGCAGTAAGTATACTCGACC-3' and LLM2_R: 5'-AATATAGGATCCTTATTTTTTACATTTC TCTGCG-3', for forward and reverse primers respectively. The underlined letters indicated the recognition site for *NcoI* and *BamHI*, respectively. Polymerase chain reaction (PCR) was performed with T100 ThermoCycler (Biorad) using KOD polymerase (Toyobo, Japan). All the DNA oligomers were synthesized by MACROGEN. The DNA sequencing was carried out by 1st BASE (Singapore). To clone the LLM2 orf into the expression vector, the orf was reamplified by PCR using the primers carrying recognition site for *NcoI* and *BamHI*. The PCR product was then purified by GeneHplow Geneaid (Taiwan) and then subjected to DNA digestion. FastDigest *NcoI* and *BamHI* (Thermo Scientific, USA) were employed for this purpose. For the expression vector was linearized by using the same restriction enzymes. Ligation of the DNA fragment into the expression vector was carried out using Fast DNA ligation kit. The ligation product was named pET_llm2 hereafter and used to transform *E. coli* BL21(DE3) (Novagen, USA). The growing colonies were then subjected for the colony's PCR using the T7 promoter and T7 terminator primers (Macrogen, Korea) to select the positive clones.

2.3. Recombinant type II luciferase-like monooxygenase (LLM2) expression and solubility check

E. coli BL21(DE3) carrying pET_*llm2* was cultivated in 5 mL LB broth supplemented with 50 µg/mL Kanamycin and grown for 16 h at 37 °C. On the following day, the culture was transferred into 50 mL fresh LB broth media supplemented with 50 µg/mL kanamycin. The culture was incubated at 37 °C for 3 h and when the optical density of 600 nm (OD_{600}) reached 0.5-0.6 then 1 mM isopropyl thio β-D-alactopyranoside (IPTG) was added. Before the addition of IPTG, a milliliter of culture was taken out and kept on ice for further analysis. The induced culture was then incubated at 37 °C for additional 3 h. After that, the cell was harvested by centrifugation at 8,000 g for 10 min. Cell pellets were then washed with 10 mM Tris HCl pH 8 twice to remove the remaining LB medium. The washed pellet was dissolved with 5 mL of 10 mM Tris-HCl pH 8. To check the solubility of recombinant protein cell pellet was disrupted by sonication (Taitec VP-050N, Japan). To separate the cell debris and supernatant, the solution was centrifugated at 12,000 g for 30 min and then cell debris was dissolved with 5 mL of the same buffer. All the sample was then kept at -20 °C for further analysis. After the adjustment to the appropriate concentration, all the prepared samples were then subjected for SDS-PAGE analysis (Laemmli 1970).

2.4. Refolding of insoluble recombinant type II luciferase-like Monooxygenase (LLM2)

The cell pellet of *E. coli* BL21(DE3) harboring pET_*llm2* harvested from 50 mL culture was dissolved in 10 mL of

10 mM Tris-HCl pH 8 and then disrupted by sonication at 50% for every 10 s. The procedure was repeated 10 times. The sonicated solution was then clarified by centrifugation at 12,000 g for 30 min at 4 °C. After centrifugation supernatant was discarded and the pellet was washed three times with 10 mL of 10 mM Tris HCl pH 8 containing 1% of Triton X-100. The washed cell pellet was then solubilized by 5 mL of 10 mM Tris HCl containing 6 M Guanidine hydrochloride (GdHCl) instead of urea (Machuca and Roujeinikova 2017). The supernatant was then dialyzed against 10 mM Tris-HCl pH 8 overnight. Following dialysis, the supernatant was then centrifugated at 12,000 g for 10 min to separate the soluble and insoluble fractions of the protein. The samples were then kept at 4 °C for further analysis.

2.5. Protein concentration measurements

The protein concentration of recombinant LLM2 was measured by the following formula (Pace et al. 1995):

$$c = \frac{A_{280}}{\varepsilon \times \ell'} \quad (1)$$

where A_{280} is the absorbance of the protein solution at 280 nm, ε is the molar extinction coefficient of the protein (M^{-1} cm^{-1}) and ℓ is the path length of the cuvette (cm). The $A_{280}^{0.1\%}$ value of recombinant LLM2 is of 0.98 (ε = 35995 M^{-1} cm^{-1}).

2.6. UV spectrum scanning of recombinant type II luciferase-like monooxygnenase (LLM2)

Fifty micrograms per milliliter (50 µg/mL) of recombinant LLM2 protein was prepared by dissolving the protein in 1 mL of 10 mM Tris-HCl pH 8. One hundred microliters volume of sample was then scanned for the UV spectrum using UV-Vis Spectronic (UV-1280) from 200-250 nm. The empty of 10 mM Tris-HCl pH 8 was used for the baseline scanning. The same procedure was employed for the UV spectrum scanning of unfolded recombinant LLM2, except for the addition of 6 M guanidium hydrochloride in 10 mM Tris-HCl pH 8. Each measurement was carried out in triplicates.

2.7. Thermodynamic analysis of recombinant type luciferase-like monooxygenase (LLM2)

To determine the thermodynamic properties, 50 µg/ml in 10 mM Tris-HCl pH 8 of recombinant LLM2 was incubated for 10 min at a different temperature from 25 to 70 °C. After that samples were incubated on ice for 5 min and centrifugated at 12,000 g for 5 min. The samples were then measured for the absorbance as a function of temperature at 205 nm (UV-1280). To calculate the thermodynamic parameters, it was assumed that the temperature-induced denaturation of LLM2 is the reversible two-state transition between native (N) and the denatured (D) states. For the calculation of the enthalpy at the half transition of the denaturation curve the following formula could be implemented (Poklar and Vesnaver 2000):

$$\Delta H°(T_m) = RT_m^2\left(\frac{1}{\Delta T}\right) \quad (2)$$

Since at the ΔG°(T) = 0, therefore, we could express the standard entropy of denaturation, as simply as follows:

$$\Delta S°(T_m) = \frac{\Delta H°(T_m)}{T_m} \quad (3)$$

2.8. LLM2 3D structure modeling

To model the 3D structure of LLM2, the AlphaFold2 running on Google Colab was implemented(Mirdita et al. 2022; Jumper et al. 2021). AlphaFold2 is the Artificial Intelegent (AI) based template free 3D structure protein modelling algorithm and therefore template structure is not necessary. The AlphaFold2 was run under the following condition: Searching of genetic databases was used mmseqs2. The sampling options was set at default setting as follows num_models : 5; use_ptm:checked; num_ensamble: 1; max_recycles: 3; tol: 0; is_training: unchecked; num_samples: 1. The refine structures with Amber-Relax were set to default. The best model structure was selected based on the highest pLDDT score. The structure generated was visualized by PyMol ver. 2.5.1.

2.9. Molecular docking of the cofactor into LLM2 protein

Molecular docking was carried out using Autodock Vina ver. 1.1.2 (Trott and Olson 2009; Eberhardt et al. 2021). Receptor and ligand were prepared by using AutoDock Tools (ADT) suite ver. 15.7, with the following condition (Morris et al. 2009): Receptor was cleaned from the water molecules and then added the polar hydrogen atoms and Kollman charges. The receptor was then saved as a pdbqt file. The grid box size was set at 40 × 40 × 40 and grid spacing was set at 1 A. The grid box center was set at 2.759 × 1.265 × (-1.222). The ligand was prepared by selecting the appropriate root site and then saving the ligand as a pdbqt file. The docking results were selected based on the highest affinity value or the appropriate binding site.

3. Results and Discussion

3.1. Cloning and expression of recombinant type II luciferase-like monooxygenase (LLM2)

For cloning purposes, the open reading frame of type II luciferase-like monooxygenase (LLM2) from *Priestia megaterium* PSA10 was amplified using a pair of primers designed based on the genome sequence of *P. megaterium* DSM319 (CP001982.1:2612851-2613855). By those primers, the orf of LLM2 *P. megaterium* PSA10 was successfully amplified (Fig. 1). BlastX analysis indicated that the amplified orf of LLM2 from *P. megaterium* PSA10 (Accession No. ON758760) was highly homolog to the luciferase-like monooxygenase from *P. megaterium* DSM319 with the identity of 99.7%.

To examine whether the recombinant LLM2 could be expressed in *Escherichia coli* BL21(DE3), the open reading frame of LLM2 (*llm2*) was inserted in the appropriate multiple cloning site of pET28a to produce the pET-*llm2* recombinant DNA (Supplementary material S1). The recombinant pET-*llm2* was then used to transform *E. coli* BL21(DE3) and the positive clone was then used for the expression of recombinant LLM2. In our work, the recombinant LLM2 could be successfully overexpressed in the *E. coli* system (Fig. 2a). The molecular weight of recombinant LLM2 was ±39.5 kDa when it was analyzed on 15% SDS-PAGE gel along with LMW. Solubility check analysis indicated that recombinant LLM2 was produced in inclusion body form (Fig. 2b). Several attempts such as reducing the inducer to 0.1 mM and lowering the induction temperatures, to produce the recombinant LLM2 in soluble form were not successful. Therefore, we have purified the recombinant LLM2 in inclusion body forms. The consequence of the harvesting of recombinant protein in inclusion body forms is the requirement to refold the recombinant protein following the solubilization of the inclusion body using a chaotropic agent such as guanidium hydrochloride or urea. The method has been reported previously with high successful rate in producing the refolded recombinant protein (Wingfield et al. 2014; Sherry et al. 2020).

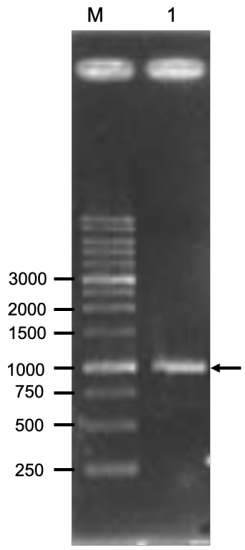

FIGURE 1 Amplified of LLM2 from the *Priestia megaterium* PSA10 genome. Visualization was caried out on 1% agarose gel electrophoresis. Lane M: 1kb DNA ladder; Lane 1. The amplified product was determined to be ±996 bp (indicated by arrow).

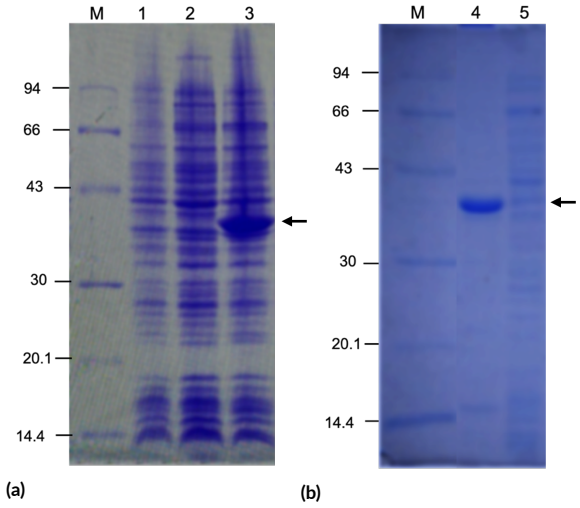

FIGURE 2 Expression and solubility analysis of recombinant LLM2 from *Priestia megaterium* PSA10 in *Escherichia coli* BL21(DE3). (a) Expression of recombinant LLM2. (b) Solubility analysis of recombinant LLM2. Lane M: Low molecular weight marker; Lane 1. Control; Lane 2. Uninduced; Lane 3. Induced; Lane 4. Cells pellet and Lane 5. Supernatant. Analysis was carried out on 15% SDS-PAGE gel. Expressed recombinant LLM2 was determined to be ±36.6 kDa (indicated by the arrow).

3.2. *Refolding of the recombinant type II luciferase-like monooxygenase (LLM2)*

To obtain the soluble recombinant LLM2 from the inclusion body of recombinant LLM2, the inclusion body was dissolved in 6 M guanidium hydrochloride (GdHCl). The solubilized inclusion body was then refolded by dialyzing the solubilized inclusion body in 10 mM Tris HCl pH 8 overnight. To test whether the refolding experiment could produce the folded recombinant LLM2, the protein from the dialyzed membrane was then subjected to centrifugation at 12,000 g for 10 min to separate the solubilized part and precipitant. The samples were then subjected to SDS-PAGE analysis and from the refolding experiments, it could be obtained almost 50% of folded recombinant LLM2 (Fig. 3a, lane 2). To further confirm whether the protein present in the solution was the fully folded recombinant LLM2, the spectrum scanning using UV range wavelength from 200 to 250 nm was carried out. The UV scanning indicated a significant difference in the spectrum behavior between the folded and unfolded recombinant LLM2 (Fig. 3b). As we can see from Fig. 3b, the spectrum of folded recombinant LLM2 exhibited the maximum peak of the spectrum at around 205 nm, while the unfolded recombinant LLM2 was not. The maximum peak at around 205 nm is due to hydrogen bond formation between backbone amides of folded protein that govern by the n→π* interactions (Bartlett et al. 2010; León et al. 2019; Saraiva 2020). The n→π* interaction is formed by the delocalization of lone pair electrons (n) from the oxygen atom to the antibonding (π*) orbital of the subsequent carbonyl group (Bartlett et al. 2010). Therefore, the results suggest that the recombinant LLM2 is in a fully folded state. Interestingly, the recombinant LLM2 could be refolded in a very simple buffer, without any addition of a reducing agent such as dithiothreitol (DTT) or β-mercaptoethanol. The amino acid composition of the LLM2 contains three (0.9%) cysteine residues which potentially form the disulphide bond during the folding process.

3.3. *Thermodynamic analysis of recombinant LLM2*

To understand the stability of the refolded recombinant LLM2 against the temperature increase, we determined

the thermodynamic parameters by calculating the change of the enthalpy (ΔH) and entropy (ΔS) of the refolded protein at the melting temperature I point (Fig. 4). The T_m value of the recombinant LLM2 was determined to be 318.3±4.4 K (Table 1), indicating that the recombinant LLM2 belongs to the mesostable proteins. Based on the T_m value, the ΔH and ΔS were determined to be 11.76±1.3 kJ.mol^{-1} and (3.74±0.48)x10^{-2} kJ.mol^{-1}.K^{-1} (Table 1), respectively. The endothermic enthalpy was due to the contribution of intramolecular hydrogen bonding (polar interactions), van der Waals interactions, and hydration effects, while the positive entropy value was due to conformational contribution over the hydrophobic hydration of unfolded protein. The thermodynamic parameters strongly suggest that the refolded recombinant LLM2 is a sufficiently stable protein.

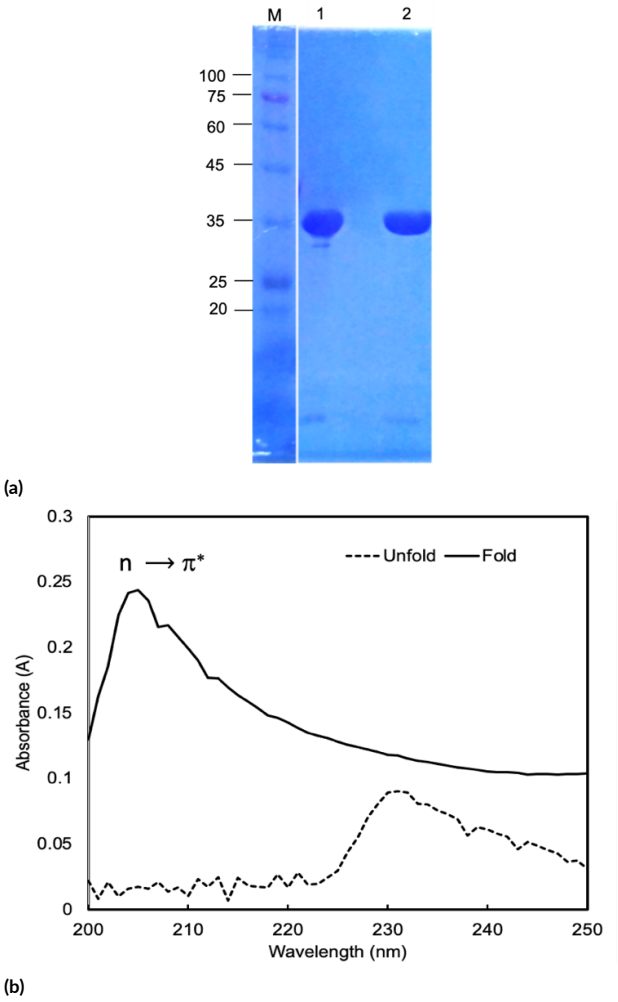

FIGURE 3 Refolding analysis of recombinant LLM2. (a) SDS-PAGE analysis; (b) Spectrum of unfolded and refolded state of recombinant LLM2. SDS-PAGE analysis was carried out on 15% SDS-PAGE gel. The folding and refolding spectrum was measured in 10 mM Tris-HCl pH 8 and 10 mM Tris-HCl with 6 M guanidium hydrochloride (GdHCl), respectively. The protein concentration used was 50 mg/ml. Lane M: Protein marker; Lane 1. Unfolded recombinant LLM2; Lane 2. Folded recombinant LLM2.

TABLE 1 Thermodynamic analysis of recombinant LLM2

Protein	Thermodynamic parameters		
	Tm (°C)	ΔH (kJ.mol^{-1})	ΔS (kJ.mol^{-1}.K^{-1})
LLM_2	318.3±4.4	11.76±1.3	(3.74±0.48)x10^{-2}

*) The thermodynamic values were measured in 10 mM Tris-HCl pH 8 at 205 nm as a function of temperature. The protein concentration was 50 µg/mL.

3.4. *Structural modeling of LLM2 3D structure and determination of flavin specificity*

To model the 3D structure of LLM2, the AlphaFold2 was implemented in this work. The 3D structure modeling of LLM2 by AlphaFold2 generates the highest pLDDT and pTM scores of 96.6 and 93.6%, respectively. The detailed quality parameters of the model are provided in the supplementary data (Supplementary material S1). LLM2 exhibits the global fold like the common luciferase protein which is characterized by the unique TIM-barrel fold (Fig. 4). The structural alignment between the LLM2 model with the MsnO8 from *Streptomyces bottropensis* (4US5) (Maier et al. 2014) and LuxA from *Vibrio harveyii* (3FGC) (Campbell and Baldwin 2009) showed that the model exhibits a highly similar fold to MsnO8 compared to that of LuxA, with the RMSD value of 0.85 Å and 9.10 Å, respectively (Fig. 5). This result correlates with the primary sequence alignment of LLM2 to MsnO8 and LuxA which exhibit the identity value of 34.97% and 15.71%, respectively (Fig. 6). Moreover, the LLM2 also contains the most conserved signature xxE43H44H45xx which is important for the interaction with the flavin molecule mainly to the isoalloxazine ring (Fig 6). As we can see that the conserved signature is located at the loop region between the β2 and α2, suggesting that the residues in the location possess a very flexible orientation. Structural examination of the conserved signature residues corroborates such findings (Fig. 5, inset). We have calculated the distortion of χ values of the residues E_{43}, H_{44}, and H_{55} of LLM2 to their corresponding residues of MsnO8 and LuxA. The distortions of χ values mostly occur at the χ_3, and χ_2, ex-

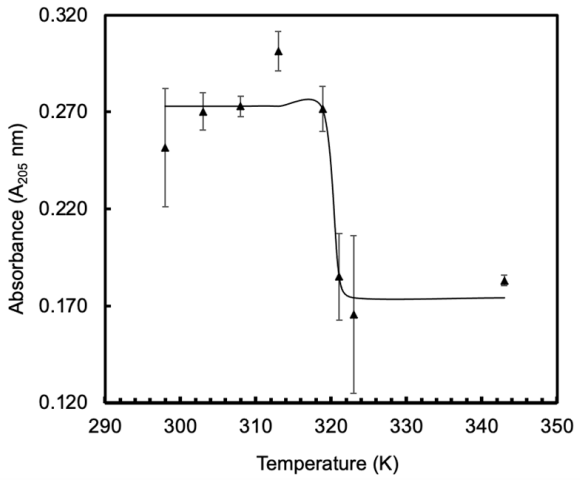

FIGURE 4 Thermal denaturation curve of recombinant LLM2. The error bars are shown as the standard deviation values (n=3).

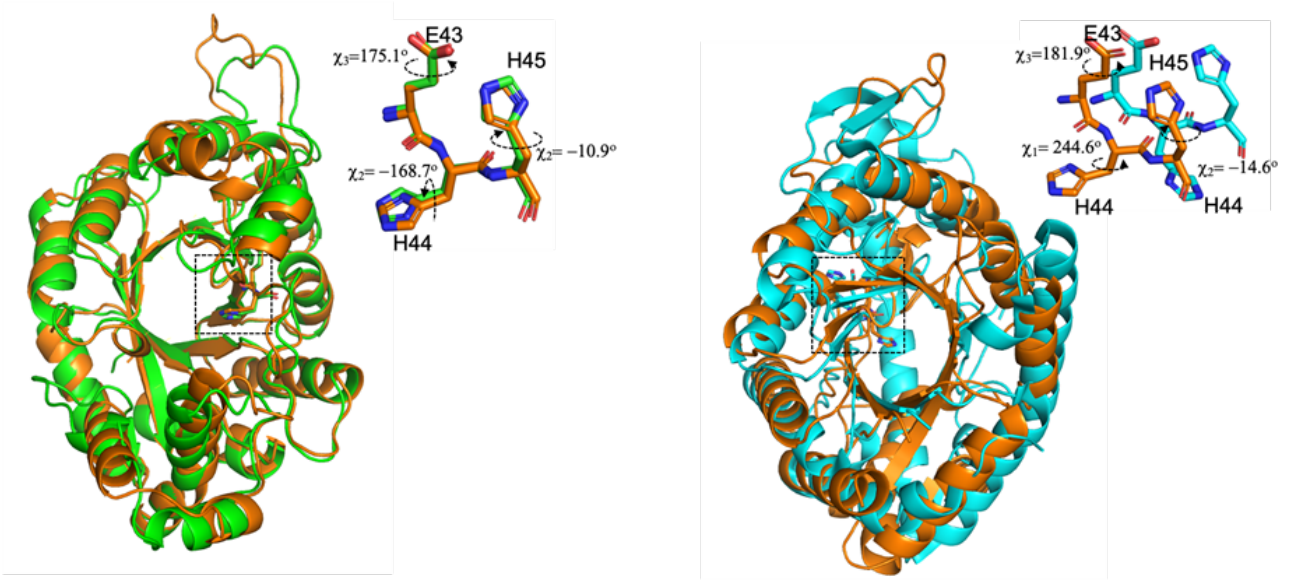

FIGURE 5 Structure of LLM2 in superposition with MsnO from *Streptomyces bottropensis* (4US5) and LuxA from *Vibrio harveyi* (3FGC). The orientation of conserved flavin binding residues of LLM2 and its χ values relative to the MsnO8 and LuxA are also shown (inset). The RMSD values of the LLM2 either to MsnO8 or LuxA are 0.85Å and 9.1Å, respectively. LLM2, MsnO8, and LuxA are indicated by orange, green, and cyan colors, respectively.

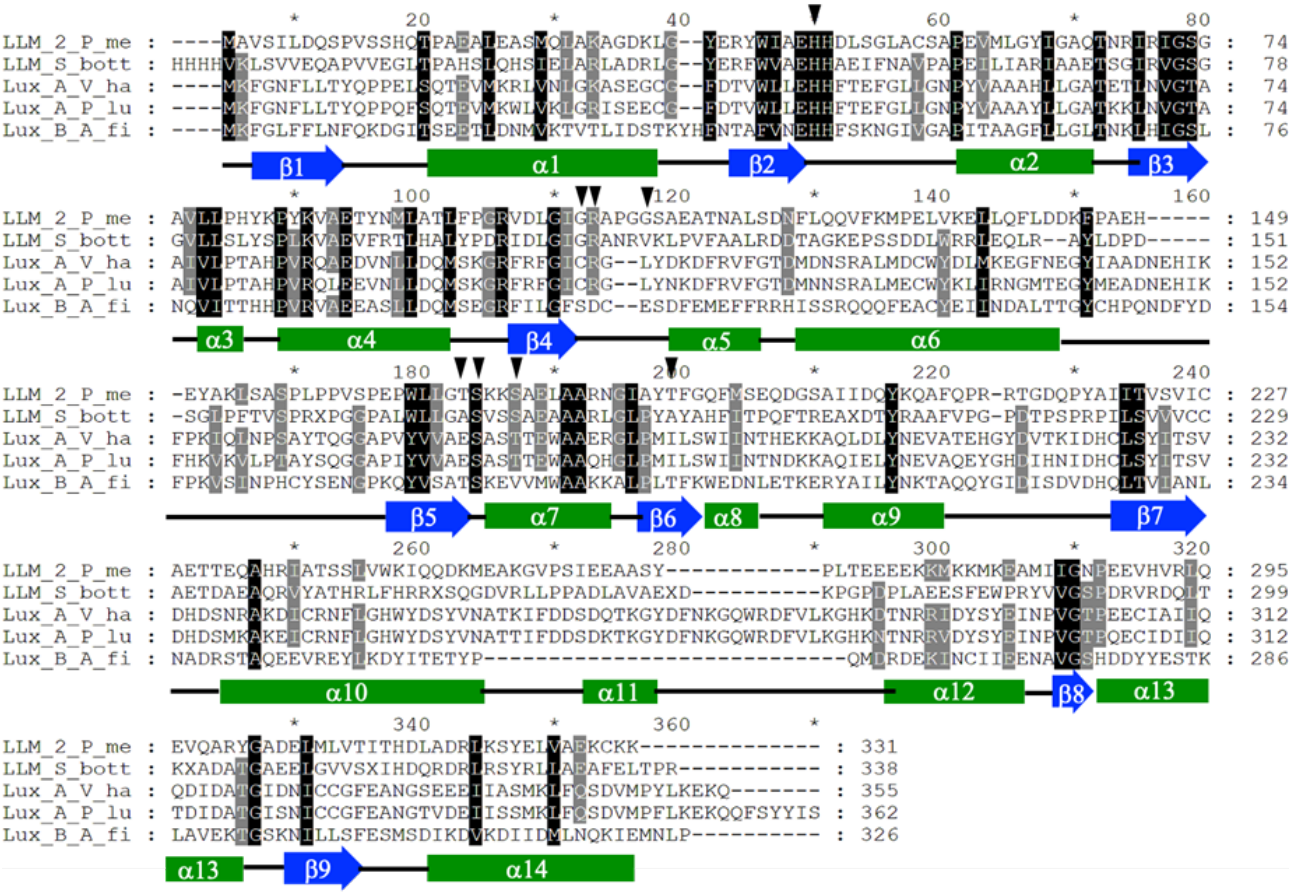

FIGURE 6 The alignment of LLM2 from *Priestia megaterium* PSA10 and its homologous. Secondary structure is shown below the sequences indicated as blue arrows and green boxes. Inverted black and red arrows indicate the possible flavin binding residues according to Lux_A from *Vibrio harveyi* (Aufhammer et al. 2005). Inverted black arrows indicate the residues that interact with the flavin molecule. LLM2_P_me: *Priestia megaterium* PSA10 (Acc. No. ON758760); LLM2_S_bott: *Streptomyces bottropensis* (Acc. No. AHL46694); Lux_A_V_ha: *Vibrio harveyi* (WP_050914092); Lux_A_P_lu: *Photorhabdus luminescent* (Acc. No. P23146; and Lux_B_A_fi : *Aliivibrio fischeri* (Acc. No. ACH64129.1).

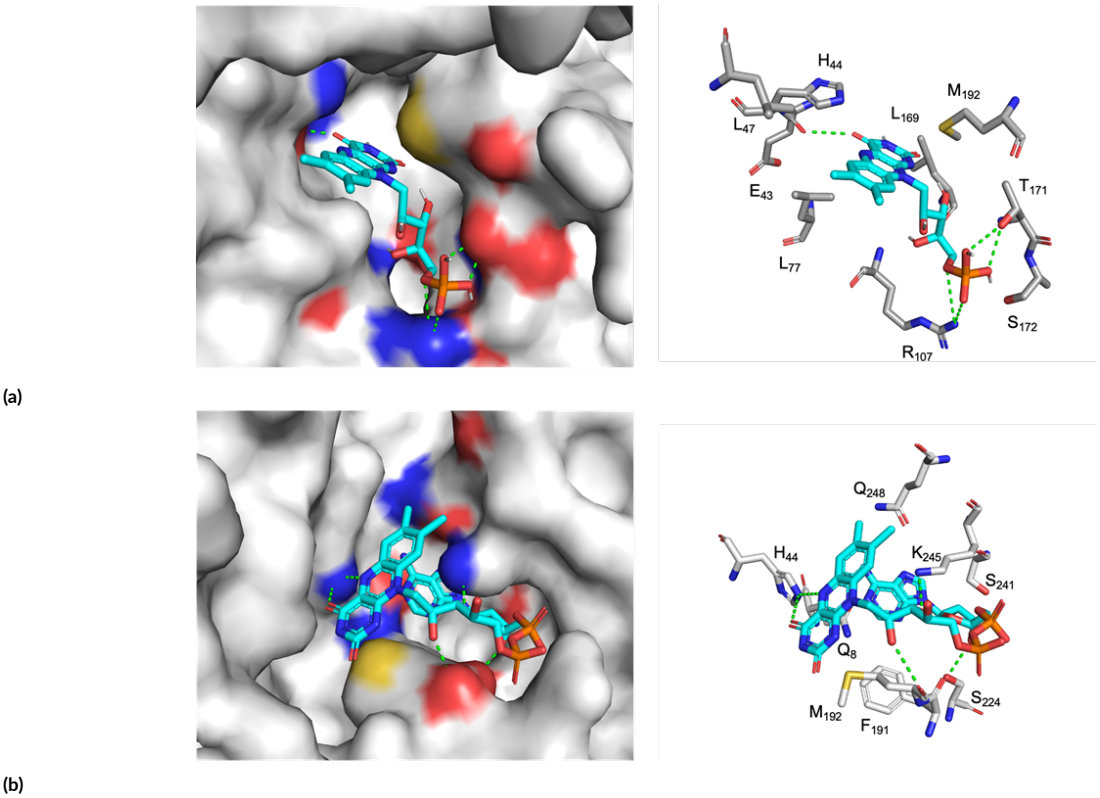

FIGURE 7 The binding mode of flavin adenine mononucleotide (FMN) (upper) and flavin adenine dinucleotide (FAD) (lower) at the binding site of LLM2. Left side shows the binding cleft of FMN and FAD, respectively, while the right side shows the residues. The binding mode shows the orientation of the isoalloxazine ring of flavin molecules to the His44 residue. The dotted green lines indicate the polar contact between the LLM2 and flavin molecule.

cept for the H_{44} that experiences the χ_1 twisting when it is compared to the corresponding residue of LuxA. The χ_3 of E_{43} twist from 175.1° to 181.9°, while the χ_2 of H_{45} distorts very little, from -10.9° to -14.6° relatives to the corresponding residues of MsnO8 and LuxA, respectively. For the E_{44} residue, the twisting of χ_2 and χ_1 is determined to be -168.7° and 244.6°, relatives to the H_{44} of MsnO8 and LuxA, respectively. To further understand the function of the LLM2 from *P. megaterium* PSA10, we have examined the interaction between the LLM2 with flavin either FMN or FAD. The binding mode was selected based on the orientation of the isoalloxazine ring of flavin molecules to the orientation of the H_{44} residue and other flavin binding residues of the protein (Fig. 6 and Fig. 7). The residues of LLM2, mainly the ones that make polar contact with FMN are only three residues, namely E_{43}, R_{107} and T_{171} that correspond to the E_{43}, R_{107}, and E_{175} of the binding residues of LuxA protein (3FGC), respectively (Fig. 7, upper). The binding affinity of the FMN on LLM2 is significantly lower compared to the one that bind to LuxA (Table 2). However, the binding mode of FAD on LLM2 and on LuxA is significantly different, as well as to the binding mode of FMN on LLM2. Four residues of LLM2 can form polar contact with FAD and surprisingly one of the residues is H_{44} (Fig. 7). The binding mode of FAD on LuxA exhibits similar orientation with FMN, mainly for the isoalloxazine ring orientation, but not at the riboflavin site. Only single residue of LuxA (W194) that make polar contact with the adenine ring of FAD (Supplementary material S1). These discrepancies are not surprisingly since the FAD has longer tail compared to the FMN. Our result also shows that the binding affinity of FAD is higher by 2 kcal.mol^{-1} compared to the FMN. Similar evidence also can be observed in the binding affinity of FAD and FMN in MsnO8 (4US5). The binding affinity of FAD in MsnO8 is 2.5 kcal. mol^{-1} higher than FMN. However, such a situation does not occur in LuxA (3FGC) in which the flavin molecules exhibit comparable binding affinity. These results indicated that the LLM2 prefers FAD for its cofactor. Our finding also suggests that LLM2 might be a unique member of group C of FMO concerning its cofactor since most of the members of group C FMO use FMN as a cofactor, instead of FAD. The group C FMO structurally contains TIM-barrel fold, and mostly use FMN as cofactor (MacHeroux et al. 2011; Paul et al. 2021). It has been reported that the flavoenzyme such as proline dehydrogenase and methyltrahydrofolate (MTHR) which have similar TIM-barrel fold does not require FMN, but FAD as cofactor (MacHeroux et al. 2011; Huijbers et al. 2017). Although the result was not surprisingly, since the cellular concentration of FAD in the cell much larger than FMN (Lienhart et al. 2013; Hühner et al. 2015; Garma et al. 2016), these results strongly suggest that the classification of the LLM as an FMN-binding enzyme should be revised.

TABLE 2 The binding affinity of FAD and FMN on the binding site of LLM2, 4US5 and 3FGC

No	Substrate	Binding affinity (kcal.mol^{-1})*)		
		LLM2	4US5	3FGC
1	FAD	-8.2	-11.0	-10.3
2	FMN	-6.2	-8.5	-10.8

*) The binding affinity was calculated with Autodock Vina ver. 1.1.2.

4. Conclusions

The recombinant LLM2 from *Priestia megaterium* PSA10 was expressed in *E. coli* BL21(DE3) system in inclusion body form and successfully refolded *in vitro*. The thermodynamic analysis showed that refolded recombinant LLM2 belongs to the mesostable protein. *In silico* analysis indicated that the LLM2 has a global fold like the common luciferase proteins indicated by the unique TIM-barrel fold. Regarding the flavin cofactor, the LLM2 prefers FAD as a cofactor compared to that of FMN. However, further experimental work is necessary to confirm the *in silico* works.

Acknowledgments

This work was fully funded by the Faculty of Agriculture Collaborations Grants No. 2084/PN/PT/2021 and No. 3350/UN1/PN/PN/PT.01.03/2022.

Authors' contributions

AFS, AT carried out the laboratory works and data collection. MSR conceived the study, analyzed the data, and wrote the manuscript. DW, SM conceived the study. All authors read and approved the final version of the manuscript.

Competing interests

All the authors declare no competing interest in this work.

References

Aufhammer SW, Warkentin E, Ermler U, Hagemeier CH, Thauer RK, Shima S. 2005. Crystal structure of methylenetetrahydromethanopterin reductase (Mer) in complex with coenzyme F 420 : Architecture of the F 420 /FMN binding site of enzymes within the nonprolyl cis -peptide containing bacterial luciferase family . Protein Sci. 14(7):1840–1849. doi:10.1110/ps.041289805.

Bartlett GJ, Choudhary A, Raines RT, Woolfson DN. 2010. n→ π* interactions in proteins. Nature chemical biology 6(8):615–620. doi:10.3389/fmolb.2020.598912.

Beaupre BA, Moran GR. 2020. N5 Is the New C4a: Biochemical Functionalization of Reduced Flavins at the N5 Position. Front. Mol. Biosci. 7:598912. doi:10.3389/fmolb.2020.598912.

Campbell ZT, Baldwin TO. 2009. Fre is the major flavin reductase supporting bioluminescence from Vibrio harveyi luciferase in *Escherichia coli*. J. Biol. Chem. 284(13):8322–8328. doi:10.1074/jbc.M808977200.

Chaiyen P, Fraaije MW, Mattevi A. 2012. The enigmatic reaction of flavins with oxygen. Trends Biochem. Sci. 37(9):373–380. doi:10.1016/j.tibs.2012.06.005.

Eberhardt J, Santos-Martins D, Tillack AF, Forli S. 2021. AutoDock Vina 1.2.0: New Docking Methods, Expanded Force Field, and Python Bindings. J. Chem. Inf. Model. 61(8):3891–3898. doi:10.1021/acs.jcim.1c00203.

Fürst MJ, Boonstra M, Bandstra S, Fraaije MW. 2019. Stabilization of cyclohexanone monooxygenase by computational and experimental library design. Biotechnol. Bioeng. 116(9):2167–2177. doi:10.1002/bit.27022.

Garma LD, Medina M, Juffer AH. 2016. Structure-based classification of FAD binding sites: A comparative study of structural alignment tools. Proteins Struct. Funct. Bioinforma. 84(11):1728–1747. doi:10.1002/prot.25158.

Ghisla S, Massey V. 1989. Mechanisms of flavoprotein catalyzed reactions. Eur. J. Biochem. 181(1):1–17. doi:10.1111/j.1432-1033.1989.tb14688.x.

Hefti MH, Vervoort J, Van Berkel WJ. 2003. Deflavination and reconstitution of flavoproteins: Tackling fold and function. Eur. J. Biochem. 270(21):4227–4242. doi:10.1046/j.1432-1033.2003.03802.x.

Hühner J, Ingles-Prieto Á, Neusüß C, Lämmerhofer M, Janovjak H. 2015. Quantification of riboflavin, flavin mononucleotide, and flavin adenine dinucleotide in mammalian model cells by CE with LED-induced fluorescence detection. Electrophoresis 36(4):518–525. doi:10.1002/elps.201400451.

Huijbers MM, Martínez-Júlvez M, Westphal AH, Delgado-Arciniega E, Medina M, Van Berkel WJ. 2017. Proline dehydrogenase from *Thermus thermophilus* does not discriminate between FAD and FMN as cofactor. Sci. Rep. 7:1–13. doi:10.1038/srep43880.

Joosten V, van Berkel WJ. 2007. Flavoenzymes. Curr. Opin. Chem. Biol. 11(2):195–202. doi:10.1016/j.cbpa.2007.01.010.

Jumper J, Evans R, Pritzel A, Green T, Figurnov M, Ronneberger O, Tunyasuvunakool K, Bates R, Žídek A, Potapenko A, Bridgland A, Meyer C, Kohl SA, Ballard AJ, Cowie A, Romera-Paredes B, Nikolov S, Jain R, Adler J, Back T, Petersen S, Reiman D, Clancy E, Zielinski M, Steinegger M, Pacholska M, Berghammer T, Bodenstein S, Silver D, Vinyals O, Senior AW, Kavukcuoglu K, Kohli P, Hassabis D. 2021. Highly

accurate protein structure prediction with AlphaFold. Nature 596(7873):538–589. doi:10.1038/s41586-021-03819-2.

Krow GR. 1993. The Baeyer-VilligerOxidation of Ketones and Aldehydes. John Wiley & Sons, Inc. doi:10.1002/0471264180.or043.03.

Laemmli UK. 1970. Cleavage of structural proteins during the assembly of the head of bacteriophage T4. Nature 227(5259):680–685. doi:10.1038/227680a0.

León I, Alonso ER, Cabezas C, Mata S, Alonso JL. 2019. Unveiling the n $\rightarrow \pi^*$ interactions in dipeptides. Commun. Chem. 2(1):1–8. doi:10.1038/s42004-018-0103-2.

Lienhart WD, Gudipati V, MacHeroux P. 2013. The human flavoproteome. Arch. Biochem. Biophys. 535(2):150–162. doi:10.1016/j.abb.2013.02.015.

MacHeroux P, Kappes B, Ealick SE. 2011. Flavogenomics - A genomic and structural view of flavin-dependent proteins. FEBS J. 278(15):2625–2634. doi:10.1111/j.1742-4658.2011.08202.x.

Machuca MA, Roujeinikova A. 2017. Method for efficient refolding and purification of chemoreceptor ligand binding domain. J. Vis. Exp. 2017(130):57092. doi:10.3791/57092.

Maier S, Pflüger T, Loesgen S, Asmus K, Brötz E, Paululat T, Zeeck A, Andrade S, Bechthold A. 2014. Insights into the bioactivity of mensacarcin and epoxide formation by MsnO8. ChemBioChem 15(5):749–756. doi:10.1002/cbic.201300704.

Massey V. 1994. Activation of molecular oxygen by flavins and flavoproteins. J. Biol. Chem. 269(36):22459–62. doi:10.1016/s0021-9258(17)31664-2.

Mirdita M, Schütze K, Moriwaki Y, Heo L, Ovchinnikov S, Steinegger M. 2022. ColabFold: making protein folding accessible to all. Nat. Methods 19(6):679–682. doi:10.1038/s41592-022-01488-1.

Morris GM, Ruth H, Lindstrom W, Sanner MF, Belew RK, Goodsell DS, Olson AJ. 2009. Software news and updates AutoDock4 and AutoDockTools4: Automated docking with selective receptor flexibility. J Comput Chem. 30(16):2785–2791. doi:10.1002/jcc.21256.

Pace CN, Vajdos F, Fee L, Grimsley G, Gray T. 1995. How to measure and predict the molar absorption coefficient of a protein. Protein Sci. 4(11):2411–2423. doi:10.1002/pro.5560041120.

Paul CE, Eggerichs D, Westphal AH, Tischler D, van Berkel WJ. 2021. Flavoprotein monooxygenases: Versatile biocatalysts. Biotechnol. Adv. 51:107712. doi:10.1016/j.biotechadv.2021.107712.

Pimviriyakul P, Chaiyen P. 2020. Overview of flavin-dependent enzymes, volume 47. Elsevier. doi:10.1016/bs.enz.2020.06.006.

Poklar N, Vesnaver G. 2000. Thermal Denaturation of Proteins Studied by UV Spectroscopy. J. Chem. Educ. 77(3):380–382. doi:10.1021/ed077p380.

Pradani L, Rohman MS, Margino S. 2020. The structural insight of class III of polyhydroxyalkanoate synthase from *Bacillus sp.* PSA10 as revealed by in silico analysis. Indones. J. Biotechnol. 25(1):33–42. doi:10.22146/ijbiotech.53717.

Renz M, Meunier B. 1999. 100 years of Baeyer-Villiger oxidations. European J. Org. Chem. 1999(4):737–750. doi:10.1002/(sici)1099-0690(199904)1999:4<737::aid-ejoc737>3.0.co;2-b.

Rohman MS. 2022. Bionformatics analysis of the Luciferase_like monooxygenase from Priestia megaterium DSM319 genome. Zenodo doi:https://doi.org/10.5281/zenodo.7151660.

Romero E, Gómez Castellanos JR, Gadda G, Fraaije MW, Mattevi A. 2018. Same Substrate, Many Reactions: Oxygen Activation in Flavoenzymes. Chem. Rev. 118(4):1742–1769. doi:10.1021/acs.chemrev.7b00650.

Saraiva MA. 2020. Interpretation of α-synuclein UV absorption spectra in the peptide bond and the aromatic regions. J. Photochem. Photobiol. B Biol. 212:112022. doi:10.1016/j.jphotobiol.2020.112022.

Sherry D, Worth R, Sayed Y. 2020. Two-Step Preparation of Highly Pure, Soluble HIV Protease from Inclusion Bodies Recombinantly Expressed in *Escherichia coli*. Curr. Protoc. Protein Sci. 100(1):e106. doi:10.1002/cpps.106.

Tinikul R, Chunthaboon P, Phonbuppha J, Paladkong T. 2020. Bacterial luciferase: Molecular mechanisms and applications, volume 47. Elsevier. doi:10.1016/bs.enz.2020.06.001.

Trott O, Olson AJ. 2009. AutoDock Vina: Improving the speed and accuracy of docking with a new scoring function, efficient optimization, and multithreading. J. Comput. Chem. p. 455–461. doi:10.1002/jcc.21334.

van Berkel WJ, Kamerbeek NM, Fraaije MW. 2006. Flavoprotein monooxygenases, a diverse class of oxidative biocatalysts. J. Biotechnol. 124(4):670–689. doi:10.1016/j.jbiotec.2006.03.044.

Wingfield PT, Palmer I, Liang SM. 2014. Folding and purification of insoluble (inclusion body) proteins from *Escherichia coli*. Curr. Protoc. Protein Sci. 2014:6.5.1– 6.5.30. doi:10.1002/0471140864.ps0605s78.